Marine Environmental Research 125 (2017) 63–72

Contents lists available at ScienceDirect

Marine Environmental Research

journal homepage: www.elsevier.com/locate/marenvrev

Differential impacts of global change variables on coastal South Atlantic phytoplankton: Role of seasonal variations

Marco J. Cabrerizo [a, b, *], Presentación Carrillo [c], Virginia E. Villafañe [a, d], E. Walter Helbling [a, d]

[a] Estación de Fotobiología Playa Unión, Casilla de Correos 15, 9103, Rawson, Chubut, Argentina
[b] Departamento de Ecología, Facultad de Ciencias, Universidad de Granada, Campus Fuentenueva s/n, 18071, Granada, Spain
[c] Instituto Universitario de Investigación del Agua, Universidad de Granada, C/ Ramón y Cajal, 4, 18071, Granada, Spain
[d] Consejo Nacional de Investigaciones Científicas y Técnicas (CONICET), Argentina

ARTICLE INFO

Article history:
Received 28 October 2016
Received in revised form
21 December 2016
Accepted 22 January 2017
Available online 24 January 2017

Keywords:
Net community production
Community respiration
PSII photochemistry
Ultraviolet radiation
Nutrient inputs
Warming
Global change

ABSTRACT

Global change is associated to the increase in temperature (T), nutrient inputs (Nut) and solar radiation in the water column. To address their joint impact on the net community production [NCP], respiration [CR] and PSII performance (Φ_{PSII}) of coastal phytoplankton communities from the South Atlantic Ocean over a seasonal succession, we performed a factorial design. For this, we used a 2 × 2 × 2 matrix set-up, with and without UVR, ambient and enriched nutrients, and *in situ* T and *in situ* T + 3 °C. The future scenario of global change exerted a dual impact, from an enhancement of NCP and Φ_{PSII} during the pre-bloom to an inhibition of both processes towards the bloom period, when the *in situ* T and irradiances were lower and the community was dominated by diatoms. The increased inhibition of NCP and Φ_{PSII} during the most productive stage of the annual succession could produce significant alterations of the CO_2-sink capacity of coastal areas in the future.

1. Introduction

Coastal areas represent a small fraction (~5%) of the total oceanic surface, however, they constitute the most productive ecosystems on Earth (Rousseaux and Gregg, 2014; Uitz et al., 2010). These areas are also considered biogeochemical hot spots because they receive large inputs of nutrients (Nut) and organic carbon from land and open ocean thus supporting high metabolism and primary production (Cloern et al., 2014). Coastal areas also present highly variable environmental conditions e.g., light, temperature (T) among others, making them particularly interesting model systems to evaluate the responses of organisms in a scenario of global change. Global change is a process largely related to human-derived activities e.g., the release of high amounts of CO_2 into the atmosphere due to industrialization (IPCC, 2013). Such atmospheric changes derive in more acidified and warmer water bodies, receiving higher levels of solar radiation (including ultraviolet radiation [UVR, 280–400 nm]) due to increased stratification of the water column (Williamson et al., 2014). In addition, due to the increasing human pressures through agriculture, livestock, and industry, higher population densities in areas close to the coast, and consequently higher waste removal (Cloern et al., 2016), coastal areas are incurring greater nutrient inputs through rivers, and these inputs expected to intensify during the next few decades (Rabalais et al., 2009).

The effects of variables associated to global change on coastal communities have been largely explored individually in both, laboratory and field studies. The validity of such approaches, however, is being challenged by recent research that reveals interactive effects among environmental variables that affect the responses as compared to the individual effects (Boyd et al., 2015, 2016). Thus, studies assessing multi-variable impacts are more appropriate as they provide more reliable information about future impacts of global change on aquatic ecosystems. For example, solar UVR is an abiotic factor that strongly influences the responses of phytoplankton under global change conditions. Although a huge body of

* Corresponding author. Departamento de Ecología, Facultad de Ciencias, Universidad de Granada, Campus Fuentenueva s/n, 18071, Granada, Spain.
E-mail addresses: mjc@ugr.es (M.J. Cabrerizo), pcl@ugr.es (P. Carrillo), virginia@efpu.org.ar (V.E. Villafañe), whelbling@efpu.org.ar (E.W. Helbling).

http://dx.doi.org/10.1016/j.marenvres.2017.01.005
0141-1136/

literature has shown the negative effects of UVR on several targets (e.g., photosystem II [Φ_{PSII}], proteins, DNA) and processes (e.g., growth, nutrients uptake, photosynthesis, respiration) (Häder et al., 2015) other studies have also found positive effects (e.g., higher photorepair of DNA, enhanced photosynthesis; Gao et al., 2007; Barbieri et al., 2002). Part of these contrasting responses, however, occurs due to the interaction of UVR with other variables In this sense, nutrient enrichment generally tends to counteract the negative effects of solar UVR exposure (Agustí et al., 2009; Harrison and Smith, 2013; Villafañe et al., 2014) therefore acting antagonistically. Increased temperature frequently acts in an antagonistic manner with UVR either on short- (e.g. Sobrino and Neale, 2007) and mid-term scales (Helbling et al., 2011). This antagonistic effect improves phytoplankton photochemical performance (Helbling et al., 2011; Villafañe et al., 2015; Wong et al., 2015), increasing growth rates (Morán et al., 2010) or even protein synthesis and nitrogen uptake (Toseland et al., 2013), especially when the tested organisms are below their optimal thermal limit.

In spite of the ecological and socio-economic importance that implies the prediction of the effects of multiple global change variables on aquatic ecosystems, up to date scarce experimental studies have considered how the interaction between UVR, Nut and T could impact on primary producers (Cabrerizo et al., 2014; Doyle et al., 2005; Durán et al., 2016). These studies have reported a wide range of effects under a multi-factor scenario, ranging from inhibition of phytoplankton growth (Doyle et al., 2005) to enhancement of photosynthesis and of excretion of organic carbon (Durán et al., 2016). One study carried by our group (Cabrerizo et al., 2014) further highlighted the species-specificity of responses under the joint effect of these variables − UVR, Nut and T. Moreover, most of the studies simulating a scenario of global change, however, have been performed during rather short periods of time, neglecting the natural environmental heterogeneity that can also alter the biological responses of phytoplankton. This is especially important, as aquatic ecosystems experience natural variations in their physical and chemical parameters, together with a temporal succession of species. Thus, and to address this gap of knowledge i.e., the responses of organisms to global change conditions tied to the natural variability of the environment, we designed experiments to quantify how a future scenario of UVR under increased Nut and T could alter the physiology of phytoplankton communities during the pre-bloom to bloom period in coastal South Atlantic Ocean waters. Thus we worked not only with communities that changed along the season but that also had different light and thermal history due to variable irradiances/mixing conditions, and *in situ* T due to the transition from fall to winter. We performed experiments during almost three months, manipulating simultaneously the Nut concentrations, T and radiation quality. Over this period, we measured the net community production [NCP], community respiration [CR] and the effective photochemical quantum yield (Φ_{PSII}) on different phytoplankton communities of Patagonian coastal waters.

Despite that between 6 and 11% of the global primary productivity occurs in the South Atlantic Basin (Rousseaux and Gregg, 2014; Uitz et al., 2010) and although Patagonian waters constitute one of the most important fishery areas of the Atlantic Ocean Basin (De Carli et al., 2012; Góngora et al., 2012), they continue to be a relatively unexplored area. The area has continuous inputs of nutrients from the river into the sea due to agricultural and urban activities (Helbling et al., 2010), and a clear bloom (dominated by diatoms, mainly *Odontella aurita*) during winter time and pre- and post-bloom periods (dominated by pico-nanoplankton cells, mainly flagellates) have also been reported for this site (Villafañe et al., 2004, 2013).

With this background in mind, our working hypothesis was that a future global change scenario will reduce the NCP and Φ_{PSII} performance, and will enhance the CR in the pre-bloom as compared to the bloom communities, as increased T will displace such communities above of the optimal growing temperatures experienced inside the annual thermal limits (17–9 °C). Thus, through our simulations of future global change conditions we tested the impacts of a multi-variable scenario on the communities varying during the seasonal succession.

2. Material and methods

2.1. Study site and sampling

Water samples were collected at the seawater side of the Chubut River estuary, in Patagonian coastal waters (Chubut Province, South Atlantic Ocean, Argentina) (Fig. 1). The experiments were done during the period April 5 to June 14, 2013, with field samples collected every week (10 experiments in total). Surface seawater (salinities > 31) samples (ca. 20 L) were collected in the afternoon-evening of the day previous to the experimentation at Egi station (43° 20.5′ S, 65° 02.0′ W) (Fig. 1) during high tide. The samples were pre-screened through a 180 μm Nitex mesh to eliminate mesozooplankton, and put into an acid-cleaned (1 N HCl) opaque container and immediately transported to the Estación de Fotobiología Playa Unión (EFPU, 10–15 min away from the sampling site) where experiments were performed as described below. Once at the laboratory, samples were pre-acclimated to the *in situ* T registered during the sampling moment or either to the *in situ* T + 3 °C overnight before being used in experimentation.

2.2. Experimental set up

The UVR × Nut × T effects on NCP, CR and Φ_{PSII} were assessed using a factorial design set up with a 2 × 2 × 2 matrix. All experimental units were run in triplicate. The original seawater sample was divided in two sub-samples that were put into two opaque containers. In one of them, the nutrients were kept under ambient conditions (i.e., without modification, as at the time of collection) whereas the other was enriched in macronutrients by 45 μM for nitrate + nitrite, 1.8 μM for phosphate, and 5.5 μM for silicate over their respective ambient concentration, simulating larger inputs by the Chubut river. Samples from these two Nut conditions were placed in 50 mL quartz round vessels, 24 for oxygen and 24 for Φ_{PSII} measurements, and exposed to: a) two radiation treatments, PAB (UVR + PAR, >280 nm), uncovered vessels, and P (PAR, >400 nm) vessels covered with UV Opak 395 filter (Difegra); and, b) two T treatments (*in situ* and *in situ* + 3 °C). The increase in 3 °C represents predicted values by the end of century for South Atlantic surface waters by IPCC (2013, scenario RCP 8.5).

All vessels containing the samples were put in a rotating system, to ensure homogeneous exposures, inside an illuminated environmental chamber (Sanyo MLR-350, Japan). The chamber kept the desired temperature *in situ* or *in situ* + 3 °C constant for each experimental condition. Due to logistical limitations inside the environmental test chamber, it was first set to the *in situ* water temperature and the following day to the increased temperature. To avoid alterations in the acclimation conditions and in the physiological state of the communities, we took new samples for the *in situ* + 3 °C experiments. We found no significant differences between samples taken during two consecutive days for each experiment (data not shown). Radiation levels were provided by 10 Philips daylight fluorescent tubes for PAR and 5 Q-Pannel UVA-340 tubes for UVR. The samples were exposed to constant irradiances of 164.1, 42.8 and 0.7 W m^{-2} for PAR, UV-A and UV-B, respectively. The spectral output of the lamps was checked using a

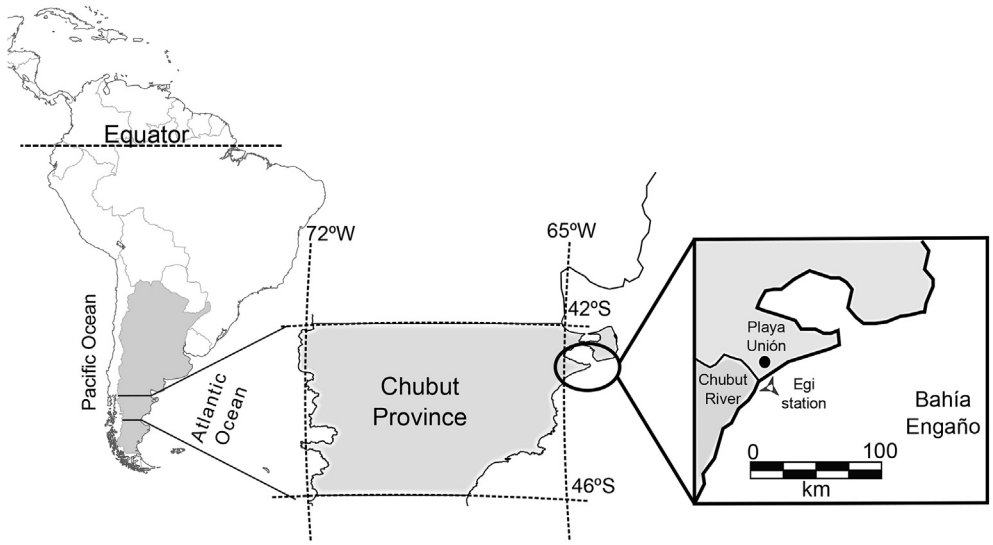

Fig. 1. Map of South America indicating the relative location of the Chubut province, Argentina. The enlarged area shows the sampling site (Egi station) outside the Chubut River estuary in Bahía Engaño.

spectroradiometer (Ocean Optics HR 2000CG-UV-NIR); no UV-C output was measured. The radiation exposure period lasted 6 h hence samples received a daily dose of 3.5 MJ m^{-2} for PAR, 910 kJ m^{-2} for UV-A and 15 kJ m^{-2} for UV-B, and the response to UVR of all samples was tested under the same conditions although the samples had a different light history (and different taxonomic composition) as the season progressed. After the exposure period, the experimental units were maintained for 8 h in darkness for respiration measurements (see below).

2.3. Analysis and measurements

2.3.1. Net community production and community respiration

Oxygen concentration was measured using an optode-probe system (Fibox 3, PreSens GmbH, Germany) equipped with fiber optics and sensor-spots (SP-PSt3-NAU-D5-YOP) together with the Oxyview 6.02 software to register the data. The system was initially calibrated using a two-point calibration for 100% and 0% oxygen saturation, at the desired temperature and at atmospheric pressure. Oxygen concentration measurements were done at the beginning of each experiment (t_0); then, every hour during the 6 h light-exposure period to determine the NCP rates. In addition, measurements of oxygen concentration were done every 30 min during the first 2 h of darkness and then every 1.5 h until finishing the 8 h dark period to determine CR rates.

2.3.2. Fluorescence measurements

Sub-samples of 3 mL were taken (with the same frequency as for oxygen concentration measurements) to measure *in vivo* chlorophyll *a* (chl *a*) fluorescence, using a pulse amplitude modulated (PAM) fluorometer (Walz, Water PAM, Effeltrich, Germany). Each sample was measured six times immediately after sampling, with each measurement lasting 10 s, therefore the total time for measuring each sample was 1 min. The effective photochemical quantum yield of PSII (Φ_{PSII}) was calculated using the equations of Genty et al. (1989) and Maxwell and Johnson (2000) as:

$$\Phi_{PSII} = \Delta F/F'_m = (F'_m - F_t)/F'_m \quad (1)$$

where F'_m is the maximum fluorescence induced by a saturating light pulse (ca. 5300 μmol photons m^{-2} s^{-1} in 0.8 s) and F_t the current steady state fluorescence induced by a red actinic light ~492 μmol photons m^{-2} s^{-1} in light-adapted cells.

2.3.3. Chlorophyll a

The chlorophyll *a* (chl *a*) content of the samples was measured by filtering two aliquots (50 mL) of the original sample onto MG-F glass fiber filters (25 mm, Munktell, Sweden) and the photosynthetic pigments were extracted in absolute methanol (Holm-Hansen and Riemann, 1978). After 1 h of extraction and 10 min of centrifugation at 2000 rpm, the supernatant was scanned (250–700 nm) using a spectrophotometer (Hewlett Packard, model 8453E, USA). The chl *a* concentration was calculated from these scans using the equation of Porra (2002).

2.3.4. Taxonomic analyses

Aliquots from the original samples were placed in 125 mL brown glass bottles and fixed with buffered formaline (0.4% final concentration of formaldehyde in the sample). Sub-samples of 25 mL were settled in a Utermöhl chamber (Hydro-Bios GmbH, Germany) for 24 h to ensure complete sedimentation of cells. The samples were counted under 200× for microplankton (>20 μm) and under 400× magnification for nanoplankton cells (<20 μm); a drop of Rose Bengal was added to the sample to better distinguish between organic material and detritus. Species were identified and enumerated using an inverted microscope (Leica, model DM IL, Germany) following the technique described in Villafañe and Reid (1995). The biovolumes of the phytoplankton cells groups analyzed were calculated following Hillebrand et al. (1999). Biovolumes were converted into carbon content (i.e., biomass) using the equations of Strathmann (1967).

2.3.5. Solar radiation, temperature and conductivity

Incident solar radiation was continuously monitored using an European Light Dosimeter Network broadband filter radiometer (ELDONET, Real Time Computers, Germany) that measures UV-B (280–315 nm), UV-A (315–400 nm) and PAR (400–700 nm) every second and averages the data over a 1 min interval. The radiometer is permanently installed on the roof of the Estación de Fotobiología Playa Unión and is calibrated every year using a clear sky solar calibration procedure together with model outputs (Björn and Murphy, 1985). Seawater temperature and conductivity was

measured for every field sampling day using a multiparameter probe (Yellow Spring Instruments, model 600 XLM, USA).

2.4. Data and statistical analyses

NCP and CR rates were calculated as the slope of the regression fit of increases (for NCP, light period) and decreases (for CR, dark period) in the oxygen concentration versus time. As the community structure and species changed along the study period, we normalized the NCP and CR rates (in μmol O_2 L^{-1} h^{-1}) by the chl *a* concentration to be able to compare the oxygen rates (in μmol O_2 μg chl a^{-1} h^{-1}).

Inhibition (*k*, in h^{-1}) and recovery (*r*, in h^{-1}) rates of Φ_{PSII} were estimated by applying an exponential regression fit to the data obtained during the light or dark periods, respectively, as:

$$\Phi_{PSII} = A \times e^{bt} \quad (2)$$

where Φ_{PSII} is the effective photochemical quantum yield of PSII, A is a constant, b is either the inhibition (*k*) or the recovery (*r*), and t is the time (in hours).

We calculated the single effects of UVR, Nut and T on NCP, CR, *k* and *r* as:

$$\text{Single effect } (\%) = \left(\text{control} - \text{variable}_{\text{single}}\right) \Big/ (\text{control}) \times 100 \quad (3)$$

where the control represents samples under the P treatment, ambient nutrient and *in situ* temperature in all cases, and variable$_{single}$ represents:(i) samples under the PAB treatment, ambient nutrient and *in situ* temperature for UVR effects, (ii) samples under the P treatment, enriched nutrients and *in situ* temperature for Nut enrichment effects and, (iii) samples under the P treatment, ambient nutrients and *in situ* temperature + 3 °C for increased T effects.

The interactive effect of UVR × Nut × T on NCP, CR, *k* or *r* rates were calculated as:

$$\text{Interactive effect } (\%) = \left(\text{control} - \text{variable}_{\text{multiple}}\right) \Big/ (\text{control}) \times 100 \quad (4)$$

where the control represents samples under the P treatment, ambient nutrient and *in situ* temperature, and the variable$_{multiple}$ represents samples under the PAB treatment, enriched nutrients and *in situ* temperature + 3 °C treatments. Error propagation was used to calculate the variance of single and interactive effects (%). The single and interactive effects on *k* and CR were multiplied by −1; thus, negative values represent an enhancement whereas positive values an inhibitory effect on the process considered.

A four-way ANOVA were used to determine differences on NCP, CR and Φ_{PSII} performance (as *k* and *r*) rates with UVR, Nut and T and sampling days (Date) as factors. Assumptions of normality and homoscedasticity were checked for each data set before ANOVA application (Zar, 1999). When significant differences were determined, a Bonferroni *post hoc* test's was performed. Due to the multiple comparisons possible between treatments for NCP, CR, *k* and *r* rates it was impractical to add all symbols in the figures to denote significances; hence they are mentioned in the text only when it is appropriate.

We used forward stepwise multiple linear regression (MLR) analyses to assess the relative strength of abiotic (i.e., *in situ* T and previous light history) and biotic variables (i.e., biomass of diatoms and flagellates) to explain the variability observed in the single and interactive effects of UVR, Nut and T on NCP, CR, *r* and *k* rates over the experimental period. The previous light history received by the communities was assessed as the mean daily solar irradiance of the previous 5–7 days of the sampling day, as this period has been shown enough for acclimation of the cells (Buma et al., 2009). Previous to the MLRs analyses, assumptions of linearity were verified through residual analyses. Multicollinearity among independent variables was also verified by correlation analysis and controlled by specifying 0.6 as the minimum acceptable tolerance; homoscedasticity was verified through normal probability scatterplot analysis.

3. Results

3.1. Seasonal physical and biological conditions

The study period was characterized by variable radiation conditions, although with a predominance of cloudy days. Also, a characteristic trend of decreasing daily doses over time was determined, from 5.39 to 1.97 MJ m^{-2}, 0.72 to 0.24 MJ m^{-2} and 14.14 to 3.10 kJ m^{-2}, for PAR, UV-A and UV-B, respectively (Fig. 2A and B). The mean daily irradiances during this period varied between ~111 and 33 (Fig. 2C), ~13-4 and 0.30–0.04 W m^{-2} (Fig. 2D) for PAR, UV-A and UV-B, respectively.

Seawater temperature, chl *a* and the biomass of the different phytoplankton groups (Fig. 3) also varied during the study period. Temperature continuously decreased from 16.9 °C in early April to 9.8 °C in mid-June (Fig. 3A). Although chl *a* concentrations generally ranged between 6 and 10 μg L^{-1}, two clear peaks (i.e. 20 in late April and ~45 μg L^{-1} in late May) were found, supporting the idea of a transition from a pre-bloom (March–May) to a bloom period (late May–June). During the study period, the proportion of nanoplankton cells (<20 μm in diameter) ranged between ~15 and 72% of the total biomass (Fig. 3B). The biomass of diatoms was higher than that of flagellates, especially in the two chl *a* peaks, where it reached values of ~70 and 80 μg C L^{-1}, respectively (Fig. 3B). The dominating diatoms during these chl *a* peaks that occurred in the two different stages of the succession were mostly chains of *Thalassiosira* species (10–50 μm) in the first peak (pre-bloom), and *Odontella aurita* in the second peak (bloom). The contribution of dinoflagellates (e.g., small naked species, *Prorocentrum micans* and *Alexandrium tamarense*) was very low throughout the study period, accounting for < 1% of the total cellular biomass.

3.2. Impact of multiple global change variables on phytoplankton physiology

Overall, NCP rates (Fig. 4) were significantly higher under nutrient enrichment than under ambient treatments during the pre-bloom (Bonferroni *post hoc*, $p < 0.05$) but as the season progressed, these differences were not significant. Nevertheless, a significant UVR × Nut × T × date effect was found on NCP rates (Table 1). At the *in situ* T, NCP rates were significant lower (Bonferroni *post hoc*, $p < 0.01$) under UVR than under PAR during most of the pre-bloom (Fig. 4A), but this difference between treatments decreased towards the bloom. At the increased T (Fig. 4B), the UVR effect was lower than that observed at the *in situ* T during the pre-bloom; however, this inhibitory UVR effect increased during the bloom, particularly under enriched treatments (Bonferroni *post hoc*, $p < 0.05$). CR rates did not exhibit any clear response pattern neither under UVR, nutrient nor T treatments throughout the season, with mean CR rates being −0.12 (± 0.06) and −0.16 (± 0.09) μmol O_2 μg Chla^{-1} h^{-1} for the *in situ* T and *in situ* +3 °C, respectively.

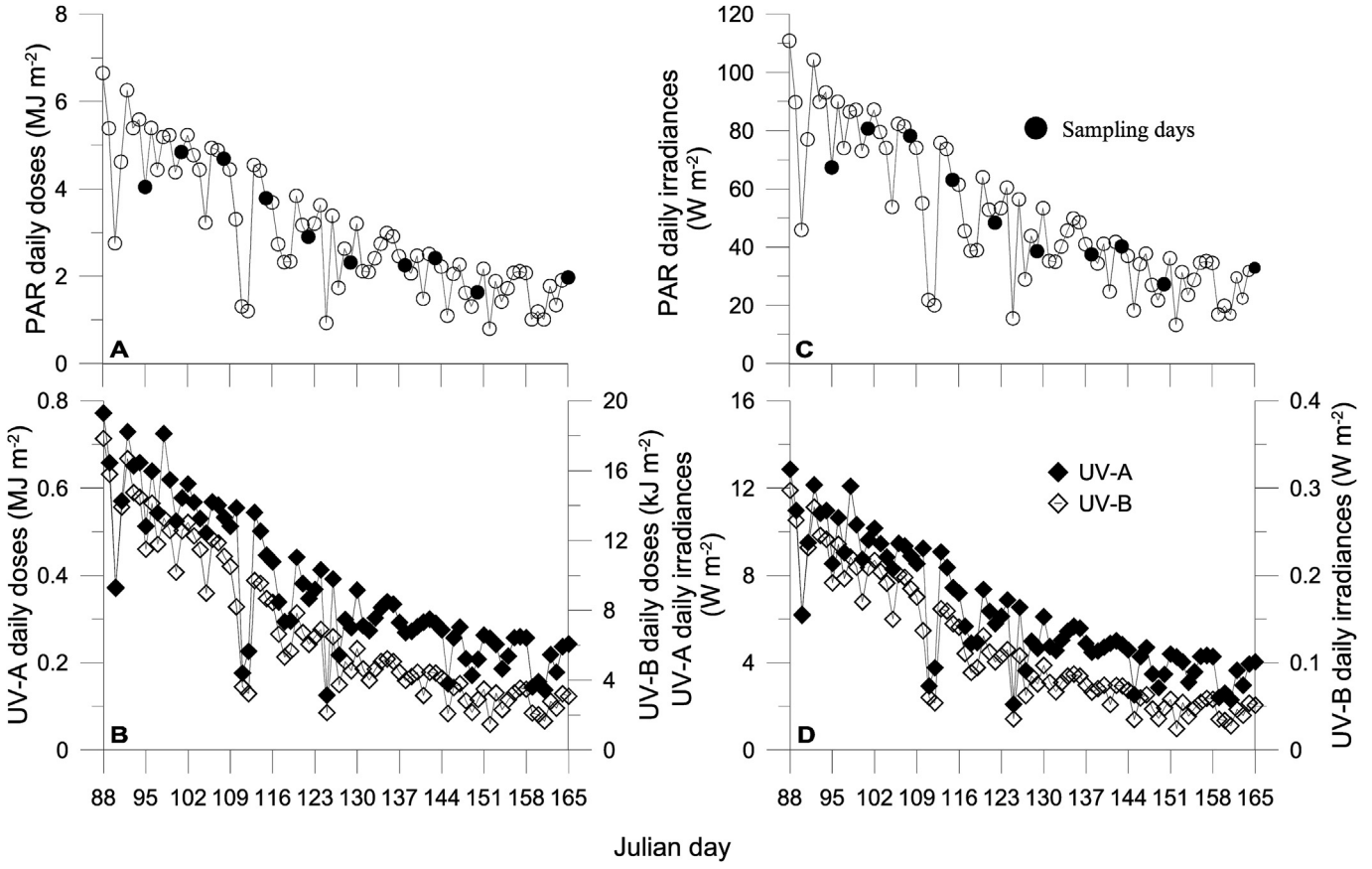

Fig. 2. Daily doses (in MJ or kJ m^{-2}) (A, B) and mean daily irradiances (in W m^{-2}) (C, D) for photosynthetically active radiation (PAR) and ultraviolet radiation A (UV-A, 315–400 nm) and B (UV-B, 280–315 nm) from Julian day 88–165. The solid circles represent the sampling days and the open circles the previous light-history of communities sampled.

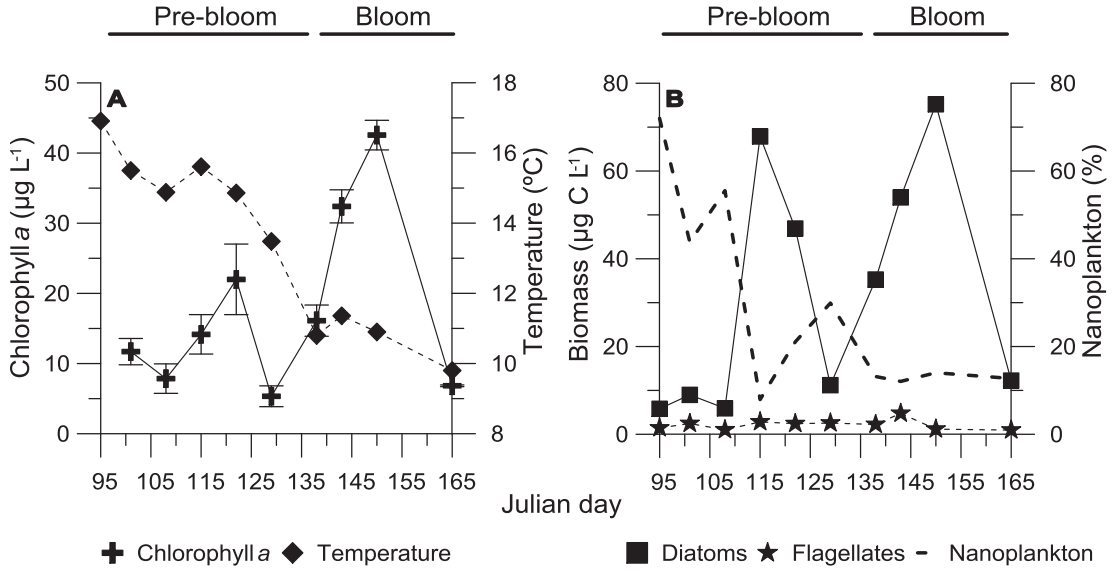

Fig. 3. Chlorophyll *a* concentration (in µg L^{-1}) and *in situ* temperature (in °C) (A); biomass of flagellates and diatoms (in µg C L^{-1}) (B), together with the percentage (%) of the nanoplankton (<µm 20) fraction during the study period.

A significant UVR × Nut × T × date interaction for Φ_{PSII} rates (Table 1) was only found on *k*. However, although *k* rates showed a slight increase during the season it was only significant towards the end of the bloom period under PAB, independently of the nutrients treatment considered at the *in situ* T, and under PAB and ambient nutrients treatment under increased temperature (Bonferroni *post hoc*, $p < 0.05$) (Fig. 5). In contrast, *r* rates did not show a clear response pattern, exhibiting similar values under all experimental conditions throughout the study period.

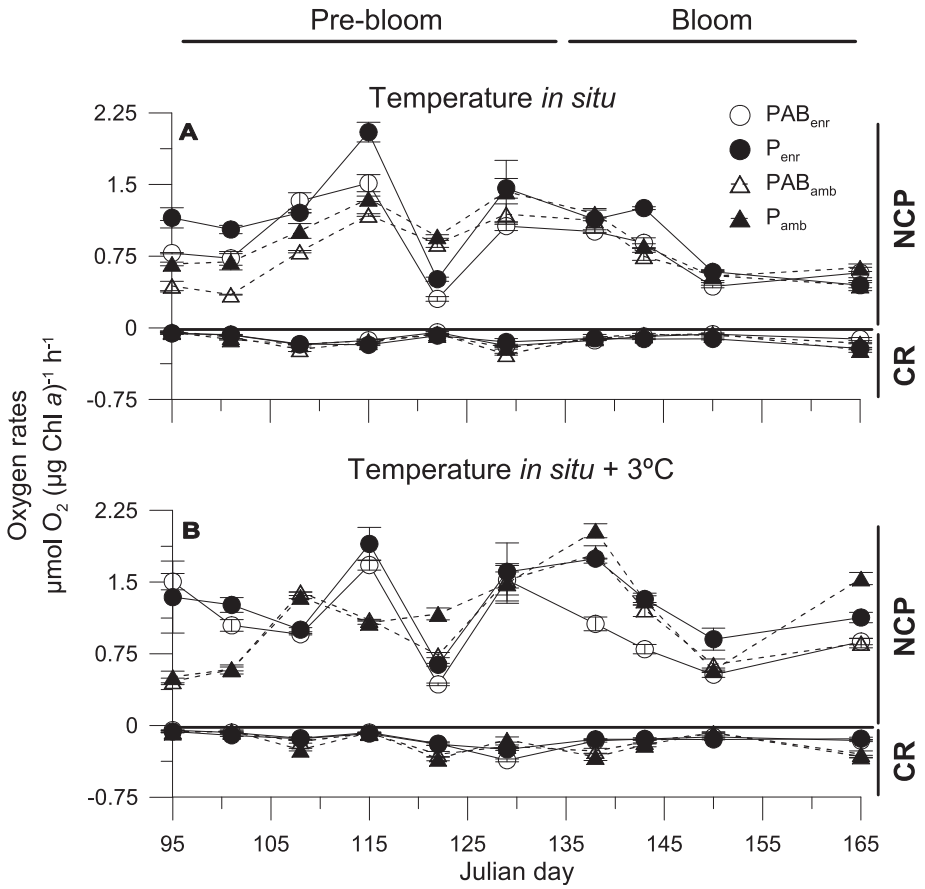

Fig. 4. Normalized net community production (NCP) and community respiration (CR) rates (in µmol O_2 µg chl a^{-1} h^{-1}) as a function of time for samples under UVR + PAR (PAB) and PAR (P), two nutrient treatments: ambient (dashed lines) and enriched (solid lines) and two temperature treatments: (A) *in situ* and (B) *in situ* + 3 °C. Each symbol represents the mean of triplicate samples whereas vertical lines indicate the standard deviation.

Table 1
Results of four-way ANOVA for the single and interactive effects of ultraviolet radiation (UVR), nutrients (Nut), temperature (T) and Date on normalized net community production (NCP) and community respiration (CR), inhibition (k) and recovery (r) rates. Significance was set at p-value < 0.05. The numbers represent the F- values, and the asterisks *, ** and *** the $p < 0.05$, $p < 0.01$ and $p < 0.001$, respectively.

	NCP	CR	k	r
UVR	73.93***	3.47**	21.24***	18.30***
Nut	117.04***	108.32***	0.17	0.11
T	168.67***	70.30***	7.69**	10.52**
Date	996.36***	1199.52***	21.01***	7.58***
UVR × Nut	0.43	2.08	12.55***	0.01
UVR × T	5.48*	1.50	1.82	2.19
UVR × Date	4.14***	20.25***	1.56	2.36*
Nut × T	3.56	10.08***	0.01	0.01
Nut × Date	90.86***	46.63***	8.41***	4.33***
T × Date	17.27***	19.34***	8.01***	4.76***
UVR × Nut × Date	3.48***	0.98	1.36	1.06
UVR × T × Date	10.52***	19.97***	0.93	1.22
UVR × Nut × T	0.73	17.85***	3.79	0.02
Nut × T × Date	44.97***	50.98***	7.14***	1.32
UVR × Nut × T × Date	4.38***	11.48	1.13**	0.71

3.3. Modeling of single and interactive effects of multiple global change variables

MLR analyses (Fig. 6, open symbols) showed that from all potential predictors assayed, only the previous light history of phytoplankton communities, the *in situ* T, and the diatom and flagellates biomass significantly explained the variability of the NCP and k. Thus, these variables were the only considered in the analysis of the modeled single and interactive effects of UVR, Nut and T on NCP and k (Table 2). The previous light history and the *in situ* T had opposite relationships (negative vs. positive coefficients, Table 2) hence both abiotic factors had an opposite impact on the magnitude of the effects of the variables tested (with the exception of UVR on NCP) and their interaction on NCP and k. Moreover, the inhibitory effect of UVR × Nut × T under the future scenario on NCP and k was increasing and significantly higher towards the bloom which matched with higher diatoms biomass (93% ± 4%) than that observed during the pre-bloom (81% ± 6%).

Overall, the inhibitory UVR effect on NCP rates decreased significantly (ca. 10%) as the seawater temperature was cooling towards the winter (Fig. 6A). The Nut effect on NCP rates (Fig. 6B) changed from a stimulation during the pre-bloom (negative values) to an inhibition towards the bloom (positive values) when the temperature decreased below 13.5 °C. The T effect (Fig. 6C) also decreased significantly as the seawater temperature decreased, resulting in inhibition of NCP rates during pre-bloom (*in situ* temperatures > 15 °C) and stimulation towards the bloom (*in situ* temperatures < 13.5 °C). The interaction of all variables studied (Fig. 6D) exerted an enhancement of NCP rates during the first half of the study period (negative values) hereafter caused an inhibitory effect under *in situ* water temperatures < 13.5 °C.

The single effect of the studied variables on k changed from negative values during the pre-bloom (temperature > 15 °C) to positive values towards the bloom (temperature < 13.5 °C) for UVR

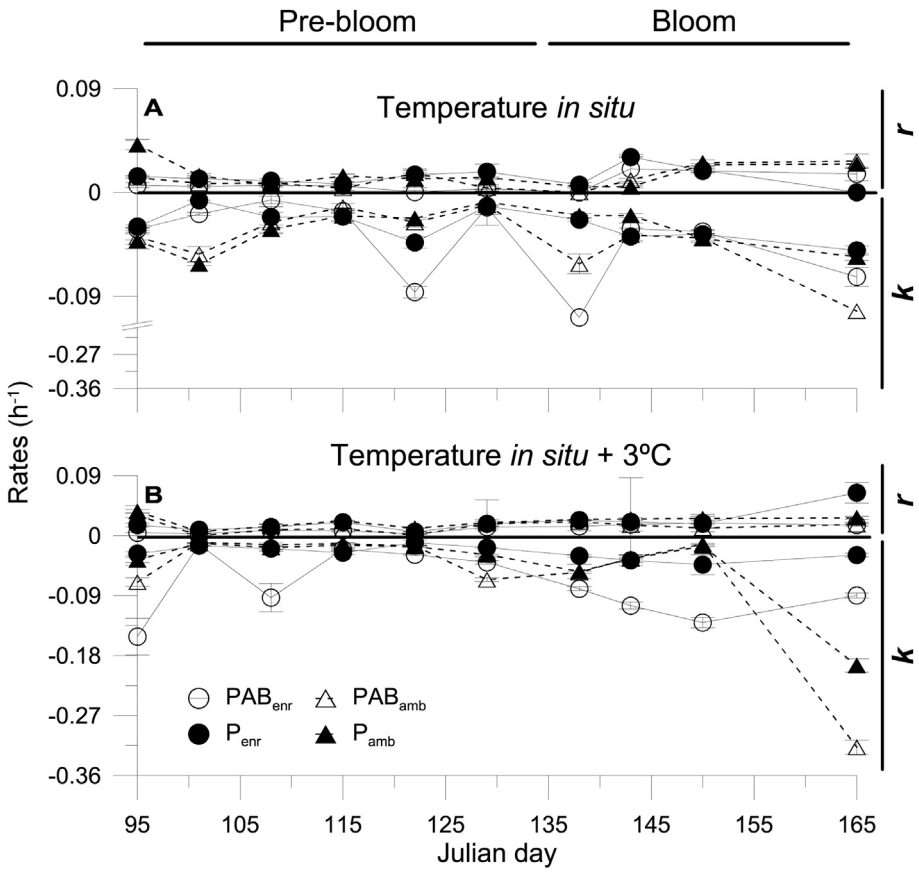

Fig. 5. Photosystem II inhibition (k) and recovery (r) rates (in h^{-1}) as a function of time for samples under UVR + PAR (PAB) and PAR (P), two nutrient treatments: ambient (dashed lines) and enriched (solid lines) and two temperature treatments: (A) *in situ* and (B) *in situ* + 3 °C. Each symbol represents the mean of triplicate samples whereas vertical lines indicate the standard deviation.

(Fig. 6E) and T (Fig. 6G) denoting higher inhibition of PSII when the *in situ* T decreased. No significant relationship was found for Nut effects as a function of the seawater temperature (Fig. 6F). The interactive effect of all factors had an increasing negative effect on k (positive values Fig. 6H) throughout the experimental period, with maximal inhibition at lower temperatures.

4. Discussion

The effects that global change variables could have on phytoplankton greatly depend on the physiological status of the cells. The changes in the community composition also need to be considered together with the differential responses of species which in turn is tied up to the environmental conditions experienced. In fact, the characteristic phytoplanktonic succession of Patagonian coastal waters with strong winter phytoplankton blooms is explained by the stability of the water column and by the shallow UML due to low wind speeds and frequencies (Helbling et al., 2005). Moreover, phytoplankton also tends to be low-light and low-temperature adapted during the winter as compared to summer or spring due to the lower incident solar irradiance penetrating the water column and the fact that the cells undergoing temperatures of ~7 °C during this stage of the year as compared with those that occurs during summer (~18 °C) (Helbling et al., 2010); thus, organisms would have higher growth under summer temperatures as compared to those occurring during winter. Therefore one cannot expect that a given variable or a combination of several of them would have the same effect throughout the year. Thus, it is not surprising that our study demonstrated that a future scenario of increased UVR, Nut and T exerts a dual impact on coastal phytoplankton as the seasonal succession progressed.

Specifically, we have found that both CR and recovery of Φ_{PSII} (r) were not significantly affected by global change variables (individually or interacting) at any time of the seasonal succession. These findings contrast with previous studies that showed that CR increased under high UVR levels (Agustí et al., 2014; Carrillo et al., 2015), nutrient inputs (Smith and Kemp, 2003) and/or warming (Yvon-Durocher et al., 2010). It is possible that the lack of a clear pattern in respiration or Φ_{PSII} (r) throughout our study could be due to a low chronic damage during the short-term exposures as reported by Heraud and Beardall (2002) and that any potential damage was quickly repaired (i.e., dynamic inhibition) as shown for diatoms under a global change condition (Cabrerizo et al., 2014).

On the other hand, the same global change variables tested here had a differential impact on NCP and Φ_{PSII} (k) at the same stage of the seasonal succession, and conversely, the impact was different when considering the same process at different times of the study period (i.e., pre-bloom vs. bloom). Contrary to our initial hypothesis, we found a positive impact, with an increase in NCP (Fig. 6D) during the pre-bloom, and a negative impact, with a significant inhibition of NCP and Φ_{PSII} during the bloom (Fig. 6H). When considering the timing of these effects, it is seen that the increasing inhibition in both physiological processes under the future conditions imposed in our study came together with a decrease in solar radiation levels, lower *in situ* T and higher dominance of large diatoms. In the following paragraphs we will discuss how the individual effects of climate change related variables changed along the season but most important, how the interactive effects of them

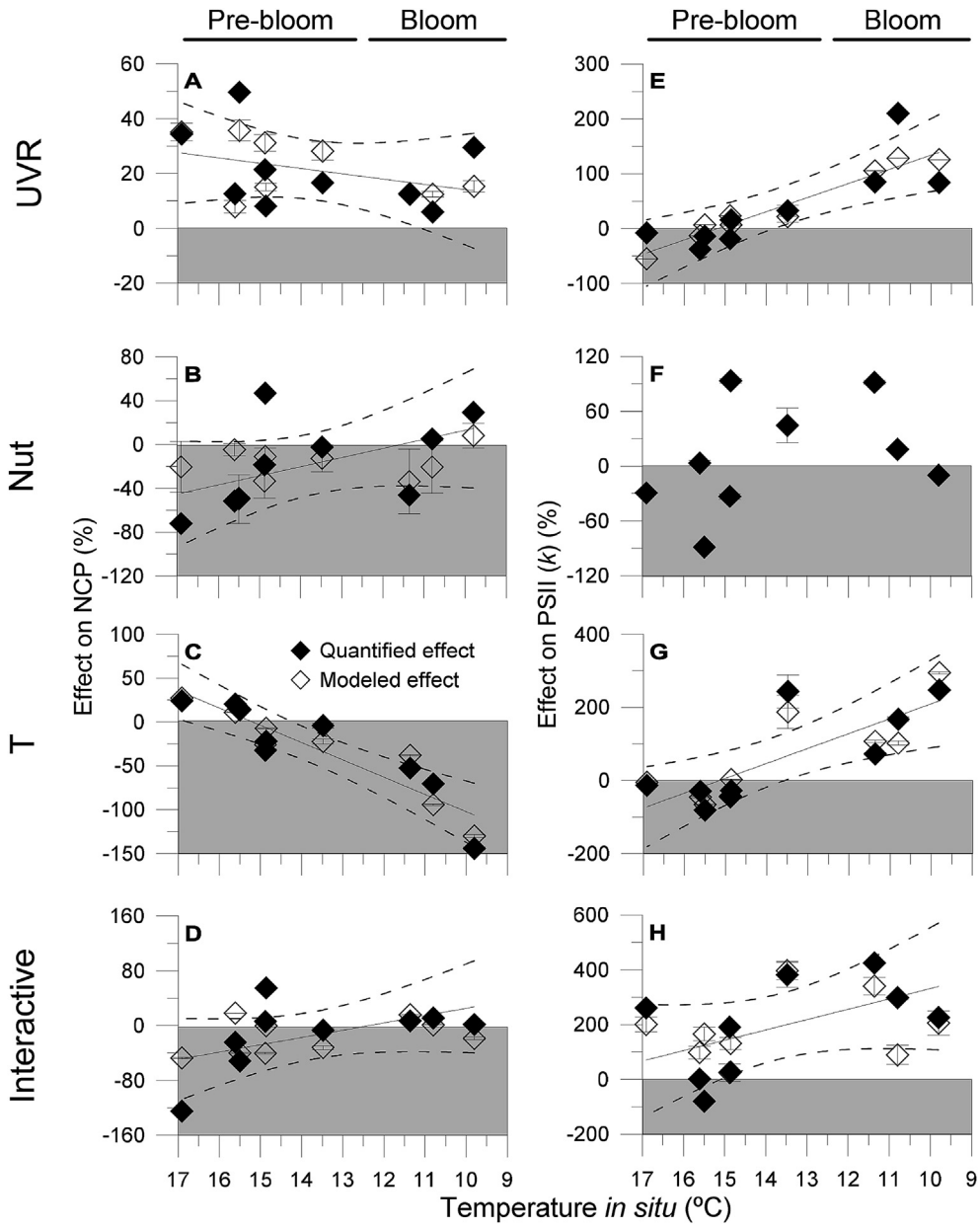

Fig. 6. Single and interactive quantified effects (solid symbols) and modeled (open symbols) by multiple linear regression for ultraviolet radiation (UVR) (A, E), nutrients (Nut) enrichment (B, F), increased temperature (T) (C, G), and their interaction on the normalized net community production (NCP) and inhibition (*k*) rates (D, H) throughout the experimental period as a function of the *in situ* temperature. The solid line indicates the regression fit for quantified effects and the dashed lines indicate the 95% confidence limits for the quantified values. Vertical lines in quantified and modeled values indicate the standard deviation calculated using error propagation. Positive values (white area) indicate an inhibitory effect and negative values (gray area) an enhancement effect. Note the different scales in the *y*-axes.

deviated or not from the single effects.

Our results show that the UVR impact on Φ_{PSII} of the pre-bloom phytoplankton community (Fig. 6E) was significantly lower than that during the bloom, and this is in agreement with previous studies assessing the effects of these wavebands on different cellular targets for photosynthesis (Helbling et al., 2011; Villafañe et al., 2013). This could be a consequence of the light acclimation towards darker conditions during the transition from fall to winter (Fig. 2) or the fact that during winter the communities are dominated mostly by diatoms instead of flagellates, which possess siliceous cell walls with optical qualities similar to quartz, and therefore, are highly transparent to UVR. Thus, a low-light acclimation together with cells highly transparent to radiation may translate as increased sensitivity to harmful effects of enhanced UVR levels, as proposed in a previous study by Llabrés and Agustí (2010). This increased sensitivity to UVR could explain the higher PSII-*k* found during the bloom than pre-bloom period. In addition, the constant radiation intensities used in our experimental set-up throughout the study period could have exacerbated the observed impact of UVR on our communities, as the UV-A and UV-B levels were higher than mean daily irradiances (Fig. 2C and D) and thus, mean daily doses received by organisms towards bloom during our exposures were between 3- (for UV-A) and 4-fold (UV-B) higher than those received in the environment (Fig. 2A and B). However, this behavior was not clearly seen in the NCP (Fig. 6A) as the inhibitory effect of UVR slightly decreased towards the bloom.

Table 2
Results of forward stepwise multiple linear regression (MLR) analysis with the best-fitting models for single (UVR, Nut and T) and interactive effects (UVR × Nut × T) on the normalized net community production (NCP) and Φ_{PSII} inhibition (k) rates. Parameters (in bold) include the daily mean photosynthetically active radiation received by communities the previous week of the experimentation (light history), diatoms and flagellates biomass, and *in situ* temperature (T), as predictor variables, whereas numbers in parentheses represent the percentage of variance explained by each predictor variable. F represents *F*-values, $^{*}p < 0.05$, $^{**}p < 0.01$ and $^{***}p < 0.001$ and R^2 determination coefficient. Note that one experimental day was excluded in all cases.

Net community production (NCP)						
	Light history	Flagellates	Diatoms	T	*F*	R^2
UVR	**0.09** (9%)	**2.95** (1%)	**−0.43** (44%)	**1.45** (1%)	38.53***	0.86
Nut	**−1.17** (27%)	**−8.18** (16%)	**−0.02** (1%)	**6.33** (1%)	3.56*	0.45
T	**−0.16** (1%)	**19.35** (19%)	**−0.32** (1%)	**21.89** (81%)	77.93***	0.93
Interactive	**0.01** (2%)	**−0.76** (3%)	**1.01** (13%)	**−3.13** (27%)	3.07*	0.45
Φ_{PSII} (k)						
UVR	**1.35** (1%)	**−4.24** (1%)	**0.70** (1%)	**−35.83** (68%)	13.38***	0.71
T	**−6.23** (5%)	**22.01** (3%)	**−4.18** (22%)	**4.89** (61%)	53.99***	0.91
Interactive	**−7.64** (13%)	**130.48** (12%)	**−7.42** (18%)	**47.85** (29%)	14.66***	0.72

Part of the differences in the UVR impact on Φ_{PSII} at different times during the seasonal succession was previously attributed to the reduced repair rates of Φ_{PSII} during the winter bloom (Villafañe et al., 2004, 2013). The increasing inhibitory effect on Φ_{PSII} towards the bloom might also partially be related to the lower *in situ* T occurring at this time of the year, due to the fact that with lower temperatures the excitation pressure on PSII tends to increase (Maxwell et al., 1995; Derks et al., 2015). One interesting point is that the increased temperature simulated in our future condition did not counteract the higher excitation pressure during the low *in situ* T period, and in fact, the inhibition of Φ_{PSII} increased towards the bloom (Fig. 6G). On the other hand, increased temperatures of the future scenario resulted in enhancement of NCP as the *in situ* T decreased (Fig. 6C), supporting the view that an increase in T was more effective at lower *in situ* T to enhance the cell metabolism, as also seen in studies carried out in marine ecosystems worldwide (García-Corral et al., 2014; Holding et al., 2013).

There was not a clear effect of Nut enrichment on Φ_{PSII} during the study period (Fig. 6F), contrasting with previous studies that showed an enhancement of Φ_{PSII} performance under such conditions (Harrison and Smith, 2013; Marcoval et al., 2007). The different responses observed between those studies and ours could be related to the fact that species need time to acclimate to the new experimental conditions whereas our short-term experimental study did not allow for such acclimation. Despite that we found no nutrient effect over the season, a recent study by Villafañe et al. (2016) in tropical coastal waters has shown that the short-term impact of nutrient addition is highly dependent on the type of community tested. For example, these authors found that diatom-dominated communities exhibited a significant increase in the Φ_{PSII} (~10%) within a few hours of nutrient addition, but when these communities were dominated by flagellates such increases in the Φ_{PSII} performance were not detected nor at mid-term scales. Still, there was a slight inhibitory effect of Nut in NCP towards the winter (Fig. 6B). In the study area, nutrient concentrations are generally high and do not seem to be a limiting factor, but this depends on the continuous riverine input (Helbling et al., 2010). However, the phytoplanktonic bloom is dominated by large diatoms (Fig. 3) that generally has low ability to uptake nutrients as compared to flagellates (Mercado et al., 2014). Besides, nutrient uptakes are T-dependent and the half-saturation constant increase with T (Litchman et al., 2015) hence it could have been reduced or, in the worst case, even inhibited under the low *in situ* T experienced by communities during the bloom. Thus it is probable that in this condition of cold *in situ* T, the increased temperature was not enough to counteract this inhibitory effect.

5. Conclusions

Overall, in the present study we call on attention to the fact that the effects of global change variables on communities should be centered not only on their interactions on diverse biological targets (e.g., oxygen-evolving complex and Φ_{PSII}) but also on the timing and length of the experimentation. This is important, as the seasonal variations concurs with global change variables conditioning the physiological status of phytoplankton and hence their responses. Although our results should be interpreted cautiously as we did not assess the potential acclimation of communities to global change variables (Yvon-Durocher et al., 2010; Villafañe et al., 2016) an increased inhibition of Φ_{PSII} performance and NCP, due to the interaction of multiple variables, during the most productive stage of the phytoplankton succession could severely alter the current key role that coastal ecosystems are playing in the global carbon cycle as CO_2 sinks.

Acknowledgements

This work was supported by Ministerio de Economía y Competitividad and Fondo Europeo de Desarrollo Regional (FEDER) (CGL2011-23681 and CGL2015-67682-R), Agencia Nacional de Promoción Científica y Tecnológica – ANPCyT (PICT 2012-0271 and PICT 2013-0208), Consejo Nacional de Investigaciones Científicas y Técnicas – CONICET (PIP N° 112-201001-00228) and Campus de Excelencia Internacional Global del Mar (CeiMar). MJC was supported by the Ministerio de Educación, Cultura y Deporte of Spain through a "Formación de Profesorado Universitario" Ph.D. grant (FPU12/01243) and a short-term placement grant (EST13/0666) and by Campus de Excelencia Internacional-Universidad de Granada (Ceibiotic – UGR, call 2015) and Fundación Playa Unión. We especially thank Cooperativa Eléctrica y de Servicios de Rawson for providing building' infrastructure. Comments and suggestions by two anonymous reviewers are greatly acknowledged. This work is in partial fulfillment of the Ph.D. thesis of MJC. This is Contribution N° 166 of Estación de Fotobiología Playa Unión.

References

Agustí, S., Duarte, C., Llabrés, M., Agawin, N.S.R., Kennedy, H., 2009. Response of coastal Antarctic phytoplankton to solar radiation and ammonium manipulation: an *in situ* mesocosm experiment. J. Geophys. Res.: Biogeosci. 114, 1–16.

Agustí, S., Regaudie-de-Gioux, A., Arrieta, J.M., Duarte, C.M., 2014. Consequences of UV-enhanced community respiration for plankton metabolic balance. Limnol. Oceanogr. 59, 223–232.

Barbieri, E.S., Villafañe, V.E., Helbling, E.W., 2002. Experimental assessment of UV effects upon temperate marine phytoplankton when exposed to variable

radiation regimes. Limnol. Oceanogr. 47, 1648–1655.
Björn, L.O., Murphy, T.M., 1985. Computer calculation of solar ultraviolet radiation at ground level. Physiol. Veg. 23, 555–561.
Boyd, P.W., Dillingham, P.W., McGraw, C.M., Armstrong, E.A., Cornwall, C.E., Feng, Y.-y., Hurd, C.L., Gault-Ringold, M., Roleda, M.Y., Timmins-Schiffman, E., Nunn, B.L., 2016. Physiological responses of a Southern Ocean diatom to complex future ocean conditions. Nat. Clim. Change 6, 207–213.
Boyd, P.W., Lennartz, S.T., Glover, D.M., Doney, S.C., 2015. Biological ramifications of climate-change-mediated oceanic multi-stressors. Nat. Clim. Change 5, 71–79.
Buma, A.G.J., Visser, R.J., Van de Poll, W., Villafañe, V.E., Janknegt, P.J., Helbling, E.W., 2009. Wavelength-dependent xanthophyll cycle activity in marine microalgae exposed to natural ultraviolet radiation. Eur. J. Phycol. 44, 515–524.
Cabrerizo, M.J., Carrillo, P., Villafañe, V.E., Helbling, E.W., 2014. Current and predicted global change impacts of UVR, temperature and nutrient inputs on photosynthesis and respiration of key marine phytoplankton species. J. Exp. Mar. Biol. Ecol. 461, 371–380.
Carrillo, P., Medina-Sánchez, J.M., Herrera, G., Durán, C., Segovia, M., Cortés, D., Salles, S., Korbee, N., Figueroa, F.L., Mercado, J.M., 2015. Interactive effect of UVR and phosphorus on the coastal phytoplankton community of the Western Mediterranean Sea: unravelling eco-physiological mechanisms. PLoS One 10, e0142987.
Cloern, J.E., Abreu, P.C., Carstensen, J., Chauvaud, L., Elmgren, R., Grall, J., Greening, H., Johansson, J.O., Kahru, M., Sherwood, E.T., Xu, J., Yin, K., 2016. Human activities and climate variability drive fast-paced change across the world's estuarine-coastal ecosystems. Glob. Change Biol. 22, 513–529.
Cloern, J.E., Foster, S.Q., Fleckner, A.E., 2014. Phytoplankton primary production in the world's estuarine-coastal ecosystems. Biogeosciences 11, 2477–2501.
De Carli, P., Braccalenti, J.C., García-de-León, F.J., Acuña-Gómez, E.P., 2012. La pesquería del langostino argentino *Pleoticus muelleri* (Crustacea: Penaeidae) en Patagonia, ¿Un único stock? An. Inst. Patagon 40, 103–112.
Derks, A., Schaven, K., Bruce, D., 2015. Diverse mechanisms for photoprotection in photosynthesis. Dynamic regulation of photosystem II excitation in response to rapid environmental change. Biochim. Biophys. Acta: Bioenergy 1847, 468–485.
Doyle, S.A., Saros, J.E., Williamson, C.E., 2005. Interactive effects of temperature and nutrient limitation on the response of alpine phytoplankton growth to ultraviolet radiation. Limnol. Oceanogr. 50, 1362–1367.
Durán, C., Medina-Sánchez, J.M., Herrera, G., Carrillo, P., 2016. Changes in the phytoplankton-bacteria coupling triggered by joint action of UVR, nutrients, and warming in Mediterranean high-mountain lakes. Limnol. Oceanogr. 61, 413–429.
Gao, K., Li, G., Helbling, E.W., Villafañe, V.E., 2007. Variability of UVR effects on photosynthesis of summer phytoplankton assemblages from a tropical coastal area of the South China Sea. Photochem. Photobiol. 83, 802–809.
García-Corral, L.S., Regaudie-de-Gioux, A., Sal, S., Holding, J., Agustí, S., Navarro, N., Mozetic, P., Duarte, C.M., 2014. Temperature dependence of planktonic metabolism in the subtropical North Atlantic Ocean. Biogeosciences 11, 4529–4540.
Genty, B.E., Briantais, J.M., Baker, N.R., 1989. The relationship between the quantum yield of photosynthetic electron transport and quenching of chlorophyll fluorescence. Biochim. Biophys. Acta 990, 87–92.
Góngora, M.E., González-Zevallos, D., Pettovello, A., Mendía, L., 2012. Caracterización de las principales pesquerías del golfo de San Jorge Patagonia, Argentina. Lat. Am. J. Aquat. Res. 40, 1–11.
Häder, D.-P., Williamson, C.E., Wängberg, S.-A., Rautio, M., Rose, K.C., Gao, K., Helbling, E.W., Sinha, R.P., Worrest, R., 2015. Effects of UV radiation on aquatic ecosystems and interactions with other environmental factors. Photochem. Photobiol. Sci. 14, 108–126.
Harrison, J.W., Smith, R.E.H., 2013. Effects of nutrients and irradiance on PSII variable fluorescence of lake phytoplankton assemblages. Aquat. Sci. 75, 399–411.
Helbling, E.W., Barbieri, E.S., Marcoval, M.A., Gonçalves, R.J., Villafañe, V.E., 2005. Impact of solar ultraviolet radiation on marine phytoplankton of Patagonia, Argentina. Photochem. Photobiol. 81, 807–818.
Helbling, E.W., Buma, A.G.J., Boelen, P., van der Strate, H.J., Fiorda Giordanino, M.V., Villafañe, V.E., 2011. Increase in Rubisco activity and gene expression due to elevated temperature partially counteracts ultraviolet radiation–induced photoinhibition in the marine diatom *Thalassiosira weissflogii*. Limnol. Oceanogr. 56, 1330–1342.
Helbling, E.W., Pérez, D.E., Medina, C.D., Lagunas, M.G., Villafañe, V.E., 2010. Phytoplankton distribution and photosynthesis dynamics in the Chubut River estuary (Patagonia, Argentina) throughout tidal cycles. Limnol. Oceanogr. 55, 55–65.
Heraud, P., Beardall, J., 2002. Ultraviolet radiation has no effect on respiratory oxygen consumption or enhanced post-illumination respiration in three species of microalgae. J. Photochem. Photobiol. B Biol. 68, 109–116.
Hillebrand, H., Dürselen, C.D., Kirschtel, D., Pollingher, U., Zohary, T., 1999. Biovolume calculation for pelagic and benthic microalgae. J. Phycol. 35, 403–424.
Holding, J.M., Duarte, C.M., Arrieta, J.M., Vaquer-Suyner, R., Coello-Camba, A., Wassmann, P., Agusti, S., 2013. Experimentally determined temperature thresholds for Arctic plankton community metabolism. Biogeosciences 10, 357–370.
Holm-Hansen, O., Riemann, B., 1978. Chlorophyll a determination: improvements in methodology. Oikos 30, 438–447.
IPCC, 2013. Climate Change. The Physical Science Basis. Cambridge University Press, New York, USA.
Litchman, E., Edwards, K.F., Klausmeier, C.A., 2015. Microbial resource utilization traits and trade-offs: implications for community structure, functioning, and biogeochemical impacts at present and in the future. Front. Microbiol. 6, 254.
Llabrés, M., Agustí, S., 2010. Effects of ultraviolet radiation on growth, cell death and the standing stock of Antarctic phytoplankton. Aquat. Microb. Ecol. 59, 151–160.
Marcoval, M.A., Villafañe, V.E., Helbling, E.W., 2007. Interactive effects of ultraviolet radiation and nutrient addition on growth and photosynthesis performance of four species of marine phytoplankton. J. Photochem. Photobiol. B Biol. 89, 78–87.
Maxwell, D.P., Falk, S., Huner, N.P.A., 1995. Photosystem II excitation pressure and development of resistance to photoinhibition. Plant Physiol. 107, 687–694.
Maxwell, K., Johnson, G.N., 2000. Chlorophyll fluorescence - a practical guide. J. Exp. Bot. 51, 659–668.
Mercado, J.M., Sala, I., Salles, S., Cortés, D., Ramírez, T., Liger, E., Yebra, L., Bautista, B., 2014. Effects of community composition and size structure on light absorption and nutrient uptake of phytoplankton in contrasting areas of the Alboran Sea. Mar. Ecol. Progr. Ser. 499, 47–64.
Morán, X.A.G., López-Urrutia, A., Calvo-Díaz, A., Li, W.K.W., 2010. Increasing importance of small phytoplankton in a warmer ocean. Glob. Change Biol. 16, 1137–1144.
Porra, R.J., 2002. The chequered history of the development and use of simultaneous equations for the accurate determination of chlorophylls a and b. Photosynth. Res. 73, 149–156.
Rabalais, N.n., Turner, R.E., Díaz, R.J., Justic, D., 2009. Global change and eutrophication of coastal waters. ICES J. Mar. Sci. 66, 1528–1537.
Rousseaux, C.S., Gregg, W.W., 2014. Interannual variation in phytoplankton primary production at a global scale. Remote Sens. 6, 1–19.
Smith, E.M., Kemp, W.M., 2003. Planktonic and bacterial respiration along an estuarine gradient: responses to carbon and nutrient enrichment. Aquat. Microb. Ecol. 30, 251–261.
Sobrino, C., Neale, P.J., 2007. Short-term and long-term effects of temperature on photosynthesis in the diatom *Thalassiosira pseudonana* under UVR exposures. J. Phycol. 43, 426–436.
Strathmann, R.R., 1967. Estimating the organic carbon content of phytoplankton from cell volume or plasma volume. Limnol. Oceanogr. 12, 411–418.
Toseland, A., Daines, S.J., Clark, J.R., Kirkham, A., Strauss, J., Uhlig, C., Lenton, T.M., Valentin, K., Pearson, G.A., Moulton, V., Mock, T., 2013. The impact of temperature on marine phytoplankton resource allocation and metabolism. Nat. Clim. Change 3, 979–984.
Uitz, J., Claustre, H., Gentili, B., Stramski, D., 2010. Phytoplankton class- specific primary production in the world's oceans: seasonal and interannual variability from satellite observations. Glob. Biogeochem. Cycl. 24, GB3016–3035.
Villafañe, V.E., Banaszak, A.T., Guendulain-García, S.D., Strauch, S.M., Halac, S.R., Helbling, E.W., 2013. Influence of seasonal variables associated with climate change on photochemical diurnal cycles of marine phytoplankton from Patagonia (Argentina). Limnol. Oceanogr. 58, 203–214.
Villafañe, V.E., Barbieri, E.S., Helbling, E.W., 2004. Annual patterns of ultraviolet radiation effects on temperate marine phytoplankton off Patagonia, Argentina. J. Plankton Res. 26, 167–174.
Villafañe, V.E., Cabrerizo, M.J., Erzinger, G.S., Bermejo, P., Strauch, S.M., Helbling, E.W., 2016. Photosynthesis and growth of temperate and sub-tropical estuarine phytoplankton in a scenario of nutrient enrichment under solar ultraviolet radiation exposure. Estuar. Coasts. http://dx.doi.org/10.1007/s12237-016-0176-z (in press).
Villafañe, V.E., Erzinger, G.S., Strauch, S.M., Helbling, E.W., 2014. Photochemical activity of PSII of tropical phytoplankton communities of Southern Brazil exposed to solar radiation and nutrient addition. J. Exp. Mar. Biol. Ecol. 459, 199–207.
Villafañe, V.E., Guendulain-García, S.D., Valadez, F., Rosiles-González, G., Helbling, E.W., Banaszak, A.T., 2015. Antagonistic and synergistic responses to solar ultraviolet radiation and increased temperature of phytoplankton from cenotes (sink holes) of the Yucatán Peninsula, México. Freshw. Sci. 34, 1282–1292.
Villafañe, V.E., Reid, F.M.H., 1995. Métodos de microscopía para la cuantificación del fitoplancton. In: Alveal, K., Ferrario, M.E., Oliveira, E.C., Sar, E. (Eds.), Manual de Métodos Ficológicos. Universidad de Concepción, Concepción, Chile, pp. 169–185.
Williamson, C.E., Zepp, R.G., Lucas, R.M., Madronich, S., Austin, A.T., Ballaré, C.L., Norval, M., Sulzberger, B., Bais, A.F., McKenzie, R.L., Robinson, S.A., Häder, D.P., Paul, N.D., Bornman, J.F., 2014. Solar ultraviolet radiation in a changing climate. Nat. Clim. Change 4, 434–441.
Wong, C.-Y., Teoh, M.-L., Phang, S.-M., Lim, P.-E., Beardall, J., 2015. Interactive effects of temperature and UV radiation on photosynthesis of *Chlorella* strains from polar, temperate and tropical environments: differential impacts on damage and repair. PLoS One 10, e0139469.
Yvon-Durocher, G., Jones, J.I., Trimmer, M., Woodward, G., Montoya, J.M., 2010. Warming alters the metabolic balance of ecosystems. Philos. T. Roy. Soc. B 365, 2117–2126.
Zar, J.H., 1999. Biostatistical Analysis, fourth ed. Prentice Hall, Englewood Cliffs, NJ.